Solid-State ^2H Quadrupole Echo NMR Characterization of Vinylene-Deuterated Poly(*p*-phenylenevinylene) Films

Jeffrey H. Simpson,† Wenbin Liang,‡ David M. Rice,† and Frank E. Karasz*,†

Department of Polymer Science and Engineering, University of Massachusetts, Amherst, Massachusetts 01003, and Department of Chemistry, Colorado State University, Fort Collins, Colorado 80523

Received November 4, 1991; Revised Manuscript Received March 4, 1992

ABSTRACT: Stretched poly(*p*-phenylenevinylene) (PPV) films in which the vinylene protons have been replaced with deuterium (PPV-d_2) have been prepared, and ^2H quadrupole echo NMR spectra have been obtained from stacked films, with their draw axes aligned relative to the NMR magnetic field. The ^2H spectra show that the orientation of the vinylene C–D bonds of PPV-d_2 is similar to that of a structure based on *trans*-stilbene. Spectra obtained at high temperature reveal substantial chain motion and are consistent with a 180° rotational jump of portions of the PPV chain about the crystallographic *c* axis. Inversion–recovery quadrupole echo spectra were obtained for these films to determine the anisotropy and magnitude of T_1. These spectra also support a chain jump model and suggest that the chain jump-rate distribution is similar to that in the phenylene rings. Both chain and ring motions are discussed in relation to the paracrystalline disorder of PPV.

Introduction

Films of poly(*p*-phenylenevinylene) (PPV) with high crystallinity and good orientation have been prepared by simultaneous stretching and elimination of a sulfonium salt precursor polymer.[1-3] These films are known to have high conductivity when doped with oxidizing agents such as H_2SO_4 or AsF_5.[4] They show good tensile strength in the draw direction.[5] PPV films have recently been investigated for their nonlinear optical (NLO) properties.[6] The structure and morphology of PPV films are of interest and have been investigated by infrared (IR) spectroscopy,[7,8] diffraction methods,[9-11] and electron microscopy.[12] These investigations have shown that PPV films contain domains of high crystallinity in which the chains assume a *trans*-stilbene-like structure but that the unit cell possesses several types of positional disorder, referred to as paracrystallinity.[10,11]

The structure of stretched PPV films has also been investigated by solid-state ^2H and ^{13}C NMR methods.[13-15] ^2H quadrupole echo NMR spectra[16-18] of a phenylene ring-deuterated PPV-d_4 have been used to characterize the crystallite orientation distribution of stretched films,[13] and in general NMR results confirm the results of IR spectroscopy, diffraction methods, and electron microscopy. ^2H spectra have also suggested two types of disorder that might be related to the paracrystallinity of PPV. In particular, the phenylene rings of PPV undergo a 180° rotational jump about the ring axis (a ring flip).[14,15] For polymers, ring flips have previously been associated exclusively with disordered, amorphous domains or boundary regions of crystalline domains.[16] For PPV, ring flips must also occur within crystallites, and it has been suggested that chain disorder (as yet unidentified) within the PPV structure makes the ring-flip motion possible.[14] Also, spectra of PPV-d_4 films have shown that the tilt of the phenylene ring with respect to the *c* axis of the unit cell deviates from the structure of stilbene by 1.5°. It has been suggested that this tilt is the result of chain disorder at crystallite boundaries or of a nonplanar PPV structure.[13]

For PPV-d_4, the 180° rotational jump of the phenylene ring about its 1,4 axis obscures direct information about chain motion. However, the ^2H line shape of a vinylene C–D bond must result directly from motion of the PPV chain itself. In this report, ^2H quadrupole echo NMR spectra are presented for stretched films of PPV that were deuterated at the vinylene proton positions (PPV-d_2; Figure 1) in order to directly observe the orientation and dynamics of the chain itself. These results suggest that portions of the PPV chain undergo a 180° rotational jump, and this hypothesis is supported by measurements of ^2H spin–lattice relaxation.

Experimental Section

Materials. Deuterated PPV (PPV-d_2) films were prepared by the precursor method as previously described, except that D_2O replaced H_2O during the polymerization step.[1-3] The labile benzyl protons of the monomer exchange with D_2O solvent to yield full deuteration of the precursor polymer.[19,20] Slow back-exchange occurred during subsequent dialysis and film casting to achieve a net deuteration of the vinylene sites of 60%, as determined by the method described in ref 21. Precursor films were stretched and eliminated by the method of either Gagnon et al.[2] or Machado et al.[3] and annealed at 300 °C for 4 h under vacuum to attain complete elimination.

Samples of unoriented PPV-d_2 ("powder" samples) were prepared from both stretched and unstretched films by cutting and were vacuum-sealed into 5-mm NMR tubes (Wilmad 506-pp cut to a 3-cm length). Oriented films were affixed to Kapton tape (CHR Industries) to preserve structural integrity during folding and at high temperature. Stacked films were aligned at an angle in the magnetic field according to previously described methods. The uncertainty is estimated to be ±5°.

Methods. ^2H NMR Spectra. ^2H quadrupole echo NMR spectra were obtained at 46 MHz in the 5-mm HP (high-power) probe of a Bruker MSL-300 NMR spectrometer with parameters as previously described.[13]

Measurements of the spin–lattice relaxation time, T_1, were obtained with a three-pulse inversion–recovery quadrupole echo pulse sequence.[16,22] For this method, a 180° inversion pulse was applied to the NMR sample and was followed after a delay by a two-pulse quadrupole echo sequence.[22,23] The data for Figures 5 and 7 were obtained near the null point (where the spectral integral passes through zero intensity). The T_1 anisotropy (frequency dependence of T_1 in the powder spectrum of the unoriented sample) could be readily observed at the null point. The intensities of the spectra used to obtain the data of Figure 6 were determined in the time domain from the height of the quadrupole echo. The 90° pulse was 2.1 μs, and the 180° pulse was 4.2 μs.

* To whom correspondence should be addressed.
† University of Massachusetts.
‡ Colorado State University.

0024-9297/92/2225-3068$03.00/0

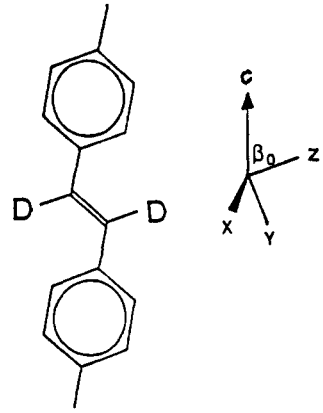

Figure 1. Structure of PPV-d_2. The principal axis system (PAS) of the vinylene C–D bond is shown. β_0 is the inclination of the vinylene C–D bond relative to the chain axis c.

Spectral curve fitting was carried out with specially written FORTRAN software that automatically selects the best-fit simulation on the basis of minimization of the residual sum of squares χ^2. The uncertainty for the phenylene–vinylene (C–D) bond orientation, β_0, was determined both by examination of χ^2 and by visual observation of frequency splittings.

Theoretical Calculation of ^{2}H Line Shapes. ^{2}H line shapes were calculated by using a specially written program that made use of the method of Wittebort et al.[24] to calculate the effects of intermediate exchange and the "method of planar moments" to calculate the effects of film orientation.[25,26] The angles and orientation functions used in the calculation of the oriented spectra of Figures 2 and 3 are similar to those used for simulation of the ^{2}H spectra of PPV-d_4 (deuterated at the phenylene ring positions).[13] The observed frequency splitting is determined by the coordinates of the magnetic field vector, $\mathbf{B}_0$, in the principal axis system (PAS) of the C–D bond and by the principal axis quadrupole tensor components, ν_{xx}, ν_{yy}, and ν_{zz} (Table I). The C–D bond PAS is related to the chain axis system (or unit cell c axis) by a rotational transformation about three Euler angles: $\mathbf{R}_1(\alpha_0,\beta_0,\gamma_0)$. Both C–D bonds of PPV-$d_2$ should have the same inclination, β_0, to the chain axis (see Figure 1; $\beta_0 = 72.3°$ for a *trans*-stilbene-like geometry).[10,11,27] Analysis of the spectra of ref 13 suggests that there is a 1.5° tilt, or disorder, of the chain direction relative to the c axis of the unit cell. This tilt is expected to affect the vinylene groups also and lead to $\beta_0 = 71.7°$, $\alpha_0 = 90°$, and $\gamma_0 = 0°$ (or $\alpha_0 = 90°$ and 270° for 2-fold jumps). The chain axis system is related to the stretching axis of the film through the transformation $\mathbf{R}_2(\alpha,\beta,\gamma)$, where α, β, and γ are angles of the powder average ($\alpha = 0$–360°, $\beta = 0$–90°, and $\gamma = 0$–360°). For oriented films, the stretching axis was related to the laboratory axis system through $\mathbf{R}_3(\theta)$, where θ is the angle between the stretch axis and the magnetic field, an experimental parameter. Chain motion at elevated temperatures was analyzed according to two possible mechanisms: either a 2-fold 180° jump or small-angle diffusion, as described later in the Results and Discussion section. Motionally averaged tensor components are referred to as ν_{XX}, ν_{YY}, and ν_{ZZ}.

Calculation of the Effects of T_1. Partially relaxed ^{2}H line shapes resulting from the inversion–recovery quadrupole echo pulse sequence were calculated by the method of Torchia and Szabo[28] as described by Wittebort et al.[24] The anisotropy of the spin–lattice relaxation time, T_1, is related to the spectral density functions J_1 and J_2 as

$$\frac{1}{T_1}(\beta,\alpha) = \frac{\omega_Q^2}{3}[J_1(\omega_0,\beta,\alpha) + 4J_2(2\omega_0,\beta,\alpha)] \quad (1)$$

$$J_m(\omega_0,\beta,\alpha) = 2\sum_{a,a'=-2}^{2} d^{(2)}_{ma}(\beta)\, d^{(2)}_{ma'}(\beta)\, d^{(2)}_{0a}(\beta_0)\, d^{(2)}_{0a'}(\beta_0)\, J_{aa'}(\omega_0,\alpha) \quad (2)$$

where α, β, α_0, and β_0 are as previously defined, ω_0 is the spectrometer frequency in radians, $m = 1$ and 2, and the values of $d^{(2)}_{aa'}$ are second-rank rotation matrix elements. For calculation of T_1, the axial asymmetry of the C–D bond quadrupole coupling is neglected and $\omega_Q = 2\pi\nu_{zz}$. The anisotropy of T_1 for a particular mechanism is determined by the spectral density functions $J_{aa'}(\omega_0)$. For the two-site jump model

$$J_{aa'}(\omega_0,\alpha) = \left(\frac{1}{4}\right)\sum_{i,j=1}^{2}(-1)^i(-1)^j \cos\,[a\Phi_i - a'\Phi_j]\left[\frac{\tau_c}{1+\omega_0^2\tau_c^2}\right] \quad (3)$$

where $\beta_0 = 71.7°$; Φ_i, $\Phi_j = \alpha + 0°$ or $\alpha + 180°$. The experimental parameter $\tau_c = 1/2k$ is the jump correlation time and is obtained directly from k, the jump rate. Equations 1–3 result from eqs 3.21 and 3.22 of Wittebort et al.[24] for the case of two-site exchange with equal populations. For the diffusion model[18,29]

$$J_{aa'}(\omega_0) = \sum_{n=1}^{N} aa'\Phi^2(\{[\cos(a\Phi)\cos(a'\Phi)(1-(-1)^n) + \sin(a\Phi)\sin(a'\Phi)(1+(-1)^n)]\}/\{[(a\Phi)^2-(n\pi/2)^2][(a'\Phi)^2-(n\pi/2)^2]\})\cos[(a-a')\alpha]\left[\frac{\tau_n}{1+\omega_0^2\tau_n^2}\right] \quad (4)$$

where $\Phi = 38°(2\pi/360°)$ and $N = 20$ is a suitable limit to the summation. Equation 4 results from the analytical solution of the diffusion equation within a square-well potential with boundaries at $\pm\Phi$ and is the spectral density function that corresponds to the correlation function shown in eqs 3.12a–c of ref 29. For eq 4, each term of the summation depends on a correlation time $\tau_n = Dn^2\pi^2/4\Phi^2$, where D is the rotational diffusion constant, an experimental parameter. Each subspectrum was scaled by the factor $(1 - 2e^{DE/T_1})$, where the delay, DE, is the recovery time

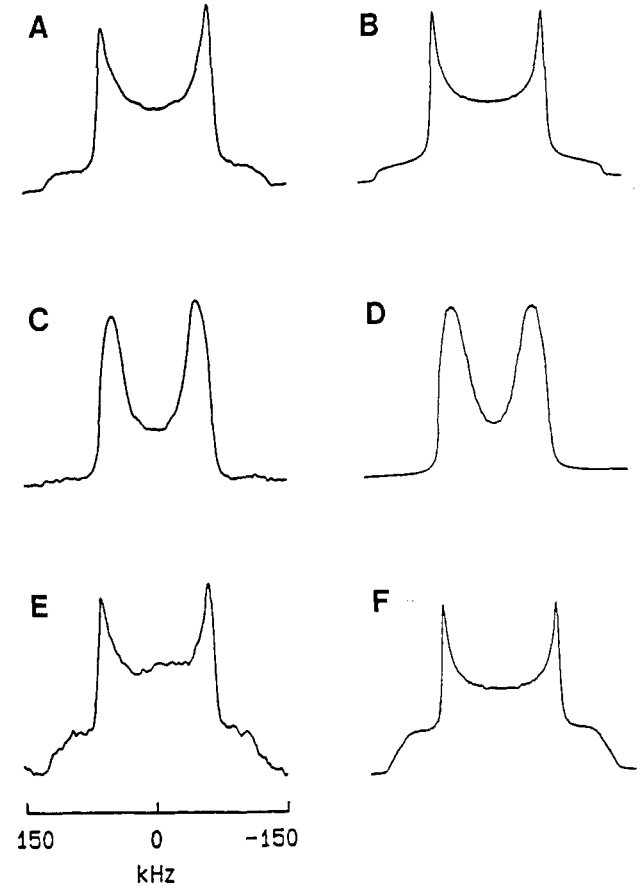

Figure 2. ^{2}H NMR spectra (A, C, and E) of PPV-d_2 obtained at 25 °C and simulations (B, D, and F). (A) A powder spectrum obtained from an unoriented film and (B) a rigid lattice simulation with PAS tensor components of Table I. (C) A spectrum obtained from a stretched film, aligned in the magnetic field ($\theta = 0°$), and (D) a simulation ($\theta = 0°$) based on the orientation distribution of ref 13. (E) A spectrum obtained from a stretched film, aligned in the magnetic field ($\theta = 90°$), and (F) a simulation ($\theta = 90°$) based on the orientation distribution of ref 13.

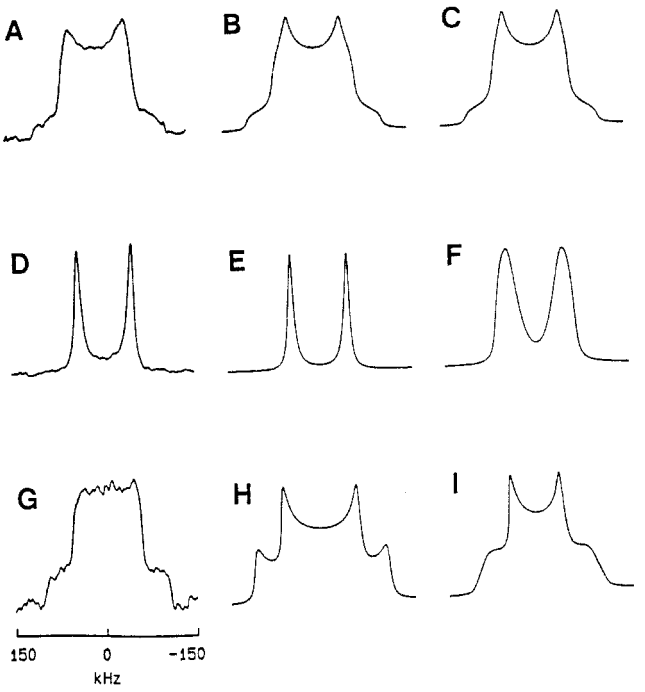

Figure 3. ^{2}H NMR spectra (A, D, and G) and simulations (B, C, E, F, H, and I) of PPV-d_2 at 225 °C. (A) A powder spectrum obtained from an unoriented film; (B) 180° jump model simulation; (C) diffusion model simulation; (D) a spectrum obtained from a stretched film, aligned in the magnetic field (θ = 0°); (E) 180° jump model simulation (θ = 0°); (F) diffusion model simulation (θ = 0°); (G) a spectrum obtained from a stretched film, aligned in the magnetic field (θ = 90°); (H) 180° jump model simulation (θ = 90°); (I) diffusion model simulation (θ = 90°).

Table I
Quadrupole Tensor Components and Coupling and Asymmetry Parameters for PPV-d_2

param	quadrupole tensor components[a] (kHz)	coupling param[b] (kHz)	asymmetry param[c]
	Static System (25 °C)		
ν_{xx}	66.5		
ν_{yy}	62.5		
ν_{zz}	-129		
$\Delta\nu_Q$		129	
η			0.03
	Motionally Averaged System (225 °C)		
ν_{XX}	58		
ν_{YY}	44		
ν_{ZZ}	-102		
$\Delta\nu_Q$		102	
η			0.14

[a] All values are ±1 kHz. The experimental frequency splitting is 2 times the tensor value. [b] $\Delta\nu_Q = |\nu_{zz}|$. [c] $\eta = (\nu_{xx} - \nu_{yy})/\nu_{zz}$.

for the inversion–recovery experiment.

Results and Discussion

^{2}H NMR Spectra of PPV-d_2 Obtained at 25 °C. Figure 2A shows a ^{2}H NMR powder spectrum obtained at 25 °C from an unstretched film with a draw ratio l/l_0 = 1 of PPV-d_2. This spectrum is characteristic of the spectrum of unoriented static C–D bonds. Figure 2B shows a simulation of Figure 2A with a quadrupole splitting $\Delta\nu_Q$ = 129 kHz and an asymmetry parameter η = 0.03. These quadrupole coupling parameters are those expected for a vinylene C–D bond with sp^2 hybridization and are also similar to, although slightly smaller than, the quadrupole coupling parameters of the phenylene ring.[13,17,25] Spectra similar to that shown in Figure 2A have also been obtained from stretched PPV-d_2 films (l/l_0 = 6) that have been mechanically disordered. Stretching does not affect the quadrupole coupling parameters of the vinylene C–D bond. A similar result was obtained for PPV-d_4.[13] Table I, rows 1–3, contains the quadrupole tensor components derived from Figure 2B and an assignment of these components to individual principal axes of the vinylene C–D bond (Figure 1). This assignment is based on the assumption that the unique tensor axis ν_{zz} is aligned with the C–D bond and that the magnitude of ν_{xx} (the component perpendicular to the sp^2 plane) is greater than that of ν_{yy}.[13]

Figure 2C shows a ^{2}H NMR spectrum obtained at 25 °C from a stretched film (l/l_0 = 6) of PPV-d_2 with its stretch axis aligned at θ = 0° to the magnetic field. Figure 2E shows a spectrum obtained with the stretch axis perpendicular to the field (θ = 90°). These spectra indicate vinylene group orientation relative to the stretch axis. Simulations of parts C and E of Figure 2 are shown in parts D and F of Figure 2 and are obtained with a chain orientation distribution similar to that previously observed for spectra of the phenylene rings of PPV-d_4.[13] Differences between the spectra of oriented PPV-d_2 and PPV-d_4 can be attributed solely to the different phenylene and vinylene C–D bond angles. Both sets of data confirm that the PPV crystalline structure is similar to that of *trans*-stilbene. For a PPV chain modeled after the *trans*-stilbene molecule,[27] the vinylene C–D bond should be oriented at β_0 = 72.3° to the chain axis. The frequency of the peaks of Figure 2C is $\pm\nu$ = 44 kHz, and β_0 can be determined from eq 5. With the values of ν_{yy} and ν_{zz} from Table I, rows 2–3

$$\nu = \nu_{zz}\cos^2\beta_0 + \nu_{yy}\sin^2\beta_0 \qquad (5)$$

gives a value for β_0 = 71.9 ± 1.0°, 1.4° below the value predicted on the basis of a *trans*-stilbene-like model. This value is consistent with the value of β_0 = 71.7 ± 0.5°, predicted from the study of oriented PPV-d_4,[13] although it is noted that the uncertainty for the value from the PPV-d_2 study is greater.

The frequency splitting for Figure 2E (θ = 90°) is determined by the tensor value perpendicular to the chain and is 3% larger than that of the powder spectrum of Figure 2A. This difference (due to the slight asymmetry of the rigid lattice coupling tensor) has also been noted for oriented PPV-d_4 and allows the assignment of the ν_{xx} of Table I, row 1, as the axis perpendicular to the vinylene plane. If ν_{yy} and ν_{xx} were interchanged, the splitting at θ = 90° would be 3% smaller.

^{2}H NMR Spectra of PPV-d_2 Obtained at 225 °C. Figure 3A shows a ^{2}H NMR powder spectrum of an unoriented PPV-d_2 film obtained at 225 °C. This spectrum is narrower than the equivalent spectrum obtained at 25 °C (Figure 2A) and has a shape with substantial axial asymmetry (η = 0.14). The narrowing can be attributed to vinylene C–D bond motion with a rate greater than the quadrupole coupling ($k > 10^6$ s^{-1}). Figure 3A is described by a set of motionally averaged quadrupole tensor components (Table I, rows 6–8). The motionally averaged ν_{YY} is assigned to the singularity of Figure 3A to provide for the consistent calculation of the asymmetry parameter. It is noted that this definition deviates from that often used for the motionally averaged axes associated with the phenylene ring flip. The assignment of axes to these tensor components depends on the mechanism of motion. The spectra of Figure 3 reveal this assignment and the mechanism of motion.

Figure 4 describes two potential mechanisms for chain motion, a 180° jump motion and a mechanism based on small-angle diffusion. Figure 4A represents a 180° rota-

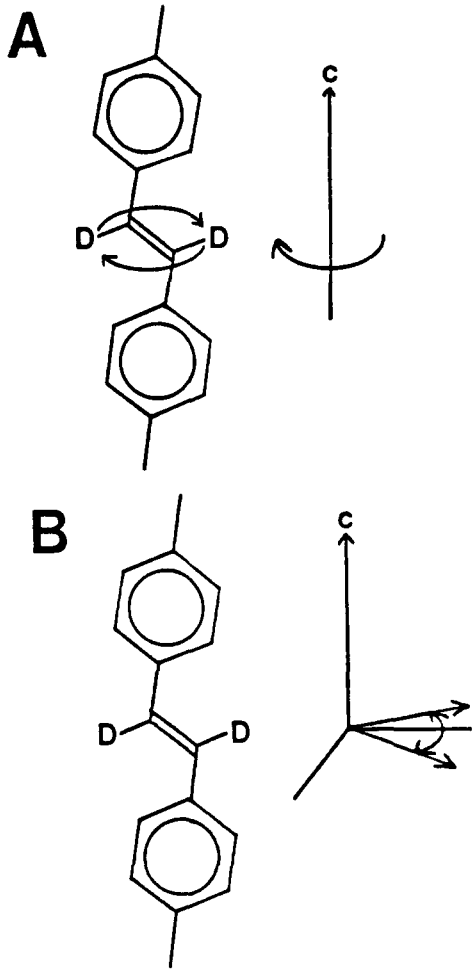

Figure 4. Two mechanisms for PPV chain motion at 225 °C. (A) 180° jump about the c chain axis. The angle of inclination of the C–D bond is constant ($\beta_0 = 71.9°$). (B) Small-angle diffusion within the boundaries of a square-well potential ($\Phi = \pm 38°$).

tional jump of the vinylene group C–D bond about the chain axis that would result from a 180° jump of portions of the PPV chain about the c axis of the unit cell, leaving the angle of inclination β_0 unchanged. Figure 3B shows a simulation resulting from such a jump motion with $\beta_0 = 71.9°$. Figure 4B shows a second mechanism based on small-angle diffusion of the C–D bond in a single potential well with square-well boundaries at $\pm\Phi$ about the chain axis. This motion might result from small-angle rotation of portions of the chain about the c axis of the unit cell (without a jump) or might approximate the cumulative result of small-angle motion about all bonds of a length of the PPV chain. A value of $\Phi = \pm 38°$ and $\beta_0 = 71.9°$ would reproduce the line shape shown in Figure 3A; the corresponding simulation is shown in Figure 3C. Both models adequately predict peak frequencies of the observed spectrum (Figure 3A). Thus powder spectra alone do not distinguish between the two mechanisms. Both simulations in parts B and C of Figure 3 also slightly overestimate the spectral width of Figure 3A. A second motion must be present in addition to jumps or diffusion.

The spectra of oriented films favor the rotational jump mechanism (Figure 4A). Parts E (jump mechanism) and F (diffusion mechanism) of Figure 3 show simulations of the spectra of the oriented PPV with $\theta = 0°$ (Figure 3D). Figure 3E reproduces the experimental frequency splitting and the narrow line width of the two individual peaks, whereas Figure 3F does reproduce the frequency splitting but not the narrow line width. For the jump model, the average ν_{YY} tensor axis (Table I, row 7) is aligned with the chain axis and ν_{XX} (Table I, row 6) is perpendicular to the sp^2 plane. The ±44-kHz frequency splitting of Figure 3D should be coincident with the peaks of Figure 3A, as is seen experimentally. For the diffusion model, the ν_{YY} tensor axis does not coincide with the chain axis. Because of this alignment, for the jump model, the quadrupole splitting should be less sensitive to crystallite misorientation than for the diffusion model, and for a chain orientation distribution with a finite width, jump spectra should have a narrower line width than spectra based on the diffusion model. The phenylene ring-flip spectrum also has this property.[15,25]

Parts H (jump mechanism) and I (diffusion mechanism) of Figure 3 show simulations of Figure 3G ($\theta = 90°$). The two pairs of edges at ±102 and ±58 kHz in Figure 3G are at the same frequencies as the corresponding edges of an unoriented sample (Figure 3A) and are similar to the ν_{ZZ} and ν_{XX} motionally averaged tensor components of Table I, rows 8 and 6, respectively. The similarity provides further evidence for the alignment of the chain axes and tensor axes, and this is a property expected for the jump mechanism. The diffusion mechanism (Figure 3I) underestimates the central splitting of Figure 3G and overestimates the outer splitting.

The slight differences noted between parts A and B of Figure 3 can be removed if additional small-angle diffusion (±20°) were present within the jump sites. In contrast, in the absence of jumps there is no simple way to modify the diffusion model to reconcile the central splitting of Figure 3I with the experimental spectrum.

The ^2H powder spectra obtained at temperatures between 25 and 225 °C have line shapes intermediate between those of the spectra of Figures 2A and 3A. No attenuation of the quadrupole echo height[17,22] is observed in this temperature range, a result suggesting that the breadth of the distribution of jump rates is large. The line shapes obtained in this temperature range are adequately reproduced by the simple superposition of fast and slow exchange limit line shapes in appropriate proportions. Because the difference between the line shapes for the fast and slow exchange limit is small and the rate distribution width is apparently large, differentiation between various potential mechanisms is not possible from the study of line shapes alone. Although the absence of attenuation could be attributed to a broad jump-rate distribution (which is expected for a polymer sample),[16] one cannot exclude a model in which the populations of the two jump sites also change with temperature. Unlike the phenylene ring, the PPV-d_2 chain does not have strict 2-fold symmetry, and the possibility of unequal jump populations must be considered.[30,31] Such a situation might arise if the intermediate exchange spectra resulted from a particular chain defect mechanism, like that observed for crystalline polymethylene chains.[32,33]

Measurement of ^2H Spin–Lattice Relaxation Time. Measurements of the magnitude and anisotropy of the spin–lattice relaxation time, T_1, have been made. These data also favor a jump mechanism rather than simple rotational diffusion and suggest that the jump motion is the result of a thermally activated change in rate, rather than being due to changing populations. For most ^2H spectra, the value of T_1 is "anisotropic";[18,22] that is, it depends on the orientation of the C–D bond relative to the magnetic field and thus depends on frequency. Like the line shape of an oriented sample, this dependence can be used to specify the mechanism of motion.

Figure 5 shows a logarithmic plot of T_1 versus inverse absolute temperature for PPV-d_2. Values of T_1 were determined from the null point of an inversion–recovery

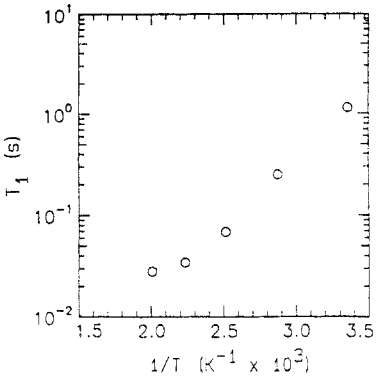

Figure 5. Logarithmic plot of spin–lattice relaxation time, T_1, of PPV-d_2 versus inverse absolute temperature. These T_1 values were obtained from the null point of an inversion–recovery quadrupole echo experiment.

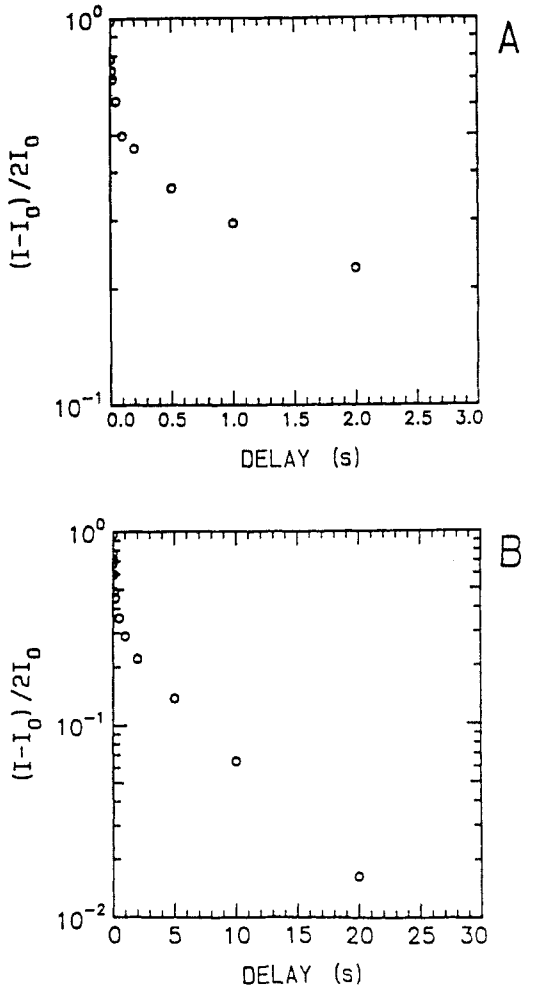

Figure 6. Logarithmic plots of scaled echo intensity $(I - I_0)/2I_0$ from an inversion–recovery quadrupole echo versus delay time (75 °C) (A) for delays between 0.0 and 2.0 s and (B) for delays up to 20.0 s.

experiment and represent the fastest relaxing deuterons at each temperature. The T_1 values decrease with increasing temperature from 1.0 s at 25 °C to 30 ms at 225 °C. At each temperature, PPV-d_2 films possess a broad distribution of T_1 values, spanning 1–2 orders of magnitude. Figure 6 shows a logarithmic plot of quadrupole echo intensity versus delay time from an inversion–recovery experiment, obtained at a single temperature (75 °C). Parts A and B of Figure 6 show the same curve with different time axes. If a single T_1 were present, these plots would be linear and the slope would be proportional to T_1. However, Figure 6 shows curvature occurring over 2 orders of magnitude, and this curvature indicates a distribution of T_1 values of similar magnitude.

The spin–lattice relaxation behavior of PPV-d_2 is consistent with a slow, large-amplitude motion. The values of T_1 in Figure 5 decrease with increasing temperature and must result from a motion with a correlation time in the nonextreme narrowing region where $\omega_0\tau_c$ is greater than unity. For ^{2}H, $\omega_0 = 2\pi(46\text{ MHz})$ and τ_c must be longer than 3.5×10^{-9} s. It has been shown that, for a 180° jump in the nonextreme narrowing region, $1/T_1$ (measured from the quadrupole echo height) is proportional to the jump rate:[22]

$$\frac{1}{T_1} = \left(\frac{2k\omega_Q^2}{5\omega_0^2}\right) \sin(2\beta_0) \tag{6}$$

for PPV-d_2, $\omega_Q = 2\pi(129\text{ kHz})$, $\omega_0 = 2\pi(46\text{ MHz})$, and $\beta_0 = 71.9°$. If the T_1 of PPV-d_2 were solely the result of a jump mechanism, then (assuming a distribution of jump rates of 2 orders of magnitude, based on Figure 5) the jump rate must be 1×10^4–1×10^6 s^{-1} at 25 °C and 5×10^5–5×10^7 s^{-1} at 225 °C.

It is useful to compare the T_1 behavior of PPV-d_2 with that of PPV-d_4.[15] The T_1 values for the phenylene rings of PPV-d_4 show a similar temperature dependence and distribution, but the values of T_1 for PPV-d_4 are about 2-fold shorter. This 2-fold difference could be due solely to the different geometries of the phenylene and vinylene bonds. Equation 6 shows that T_1 depends on the angle of inclination of the C–D bond to the jump axis and that[22]

$$\frac{T_1^{\text{vinylene}}}{T_1^{\text{phenylene}}} = \frac{\sin^2(2 \times 60.0°)}{\sin^2(2 \times 71.9°)} = 2.11 \tag{7}$$

If a thermally activated 180° jump of the PPV chain were responsible for the line shapes of PPV-d_2, then eq 7 would suggest a vinylene jump-rate distribution similar to the ring-flip jump-rate distribution.

Anisotropy of ^{2}H Spin–Lattice Relaxation. Figure 7A shows an inversion–recovery quadrupole echo NMR spectrum obtained at 225 °C for a value of the delay, DE = 12 ms, close to the null point. With this recovery time, the spectral integral is close to zero and the frequency dependence of T_1 within the spectrum is evident. The intensities at frequencies with longer T_1 are negative, and the intensities at frequencies with shorter T_1 are positive. The resulting pattern has been shown to depend on the mechanism of motion and to depend on whether $\omega_0\tau_c$ is greater or less than unity. The anisotropy of T_1 can be calculated by methods similar to those used to simulate line shapes.[18,22,24,28]

The T_1 anisotropy also supports the jump mechanism. Figure 7B shows a simulation of the spectrum of Figure 7A based on the 180° chain jump model, and Figure 7C shows a simulation of Figure 7A based on the diffusion model. For the jump mechanism, the fastest relaxation occurs at ±44 kHz, and this frequency corresponds to the motionally averaged ν_{XX}. In contrast, the diffusion model predicts that slower relaxation should occur at ±44 kHz. Both mechanisms predict the slowest relaxation near the center of the spectrum. In Figure 7A, the intensity at ±44 kHz is positive and thus supports the jump model. For the jump model, a rate of $k = 6 \times 10^7$ s^{-1} gives the best fit, a value similar to that determined from Figure 5 ($k = 5 \times 10^7$ s^{-1}). It should also be noted that the spectral intensity at ±64 kHz of Figure 7A is less than that in both parts B and C of Figure 7. This difference is attributable to the T_1 distribution. Vinylene groups with the slowest jump rates and longest T_1 contribute an inverted Pake

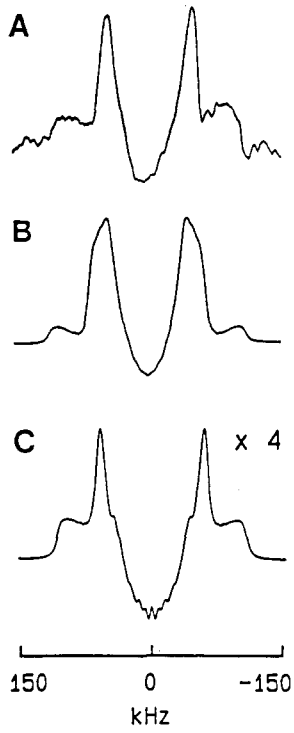

Figure 7. (A) Partially relaxed inversion–recovery quadrupole echo NMR spectrum of PPV-d_2 obtained at 225 °C with DE = 12 ms, near the null point. (B) A simulation based on a 180° jump about the chain axis (Figure 4A) ($k = 6 \times 10^7$ s^{-1}). (C) A simulation based on small-angle diffusion about the chain axis (Figure 4B).

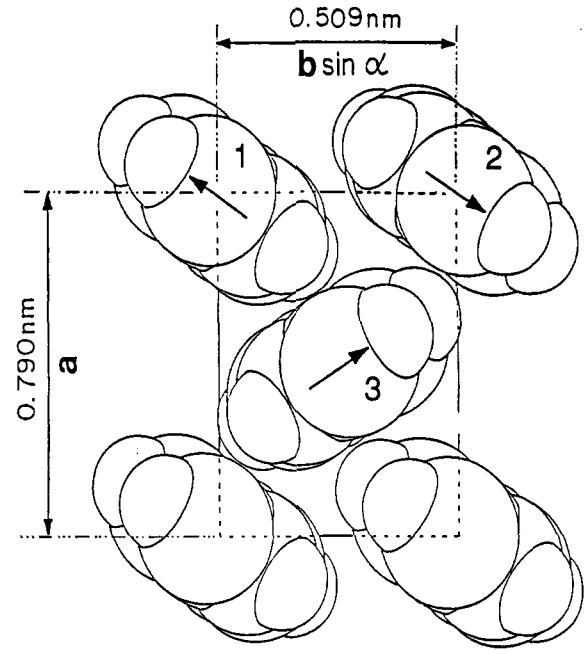

Figure 8. Projection of the PPV unit cell, showing the packing of PPV chains, perpendicular to the chain and crystallographic c axis. The a and b axes are shown. The vectors within each chain show the direction of positive phenylene ring tilt. These data suggest that the tilt direction is disordered (compare chains 1 and 2).

doublet line shape and diminish the intensity most strongly at ±64 kHz. As expected, negative peaks are observed in the null-point spectra obtained at lower temperatures (not shown), where the jump rate is close to the quadrupole coupling frequency.

NMR Data and PPV Crystalline Disorder. The simplest mechanism for a 180° chain jump within a PPV crystallite could be the coupled rotation about two phenylene–vinylene bonds located on widely spaced segments. The average PPV crystallite size is small (7 nm),[12] and such rotations could be the result of a chain defect mechanism associated with the crystallite boundaries, where greater disorder is present. A 2-fold jump should be a natural motion for the PPV chain, which itself has approximate 2-fold symmetry. For example, the high-temperature ^{19}F powder spectra of poly(tetrafluoroethylene) (PTFE) are axially symmetric and are consistent with the approximate 4-fold symmetry of the PTFE lattice site.[31]

This chain jump mechanism is consistent with earlier data obtained for PPV-d_4.[15] The spectra of PPV-d_4 are dominated by the 180° jump motion of the phenylene rings about their 1,4 axis. Additional motion of the PPV chain should cause additional fluctuations of the ring axis tilt angle of $\pm\Psi = 7.7°$, as noted in ref 13. Motion of this magnitude has a negligible effect on the ring-flip spectrum if, as observed, both motions occur on the same time scale. The two motions may in fact be coupled by a common chain defect mechanism, but current NMR data do not specify any particular mechanism unambiguously. Also, it should be noted that chain jumps of 180° alone cannot be responsible for the observed spectra of PPV-d_4.

The polymer PPV does not undergo a glass transition, nor does it undergo crystalline melting before the onset of thermal degradation upon heating.[2] Motions of the vinylene groups must result from thermally activated chain defects associated with the stable PPV crystal lattice. It is useful to compare the dynamic disorder evident in the NMR spectrum at high temperature with the static disorder that is observed for the PPV crystal structure,[10,11] so-called paracrystallinity.

Figure 8 shows a projection perpendicular to the c axis of the PPV unit cell.[10] The PPV chain itself does not have strict 2-fold symmetry because of the slight tilt of the phenylene rings relative to the chain axis, and the arrows in Figure 8 can be associated with a positive direction of phenylene ring or vinylene tilt.[13] Sites 1 and 2 in Figure 8 show two adjacent chains with opposite tilt. If the PPV chain occupies both rotational conformations with equal probability, then one must conclude that the packing interactions associated with phenylene ring tilt do not significantly affect the energy of the two conformations. Granier et al.[10,11] have noted that diffraction data do not specify the direction of phenylene ring tilt. A 180° rotation about the chain axis is the simplest disorder that could be present within the PPV unit cell. NMR data have shown that this disorder is indeed present at 225 °C, and the T_1 data suggest that it is also present at low temperature with a slower rate.

Electron diffraction has further shown that there is a lack of axial registry between the chains of adjacent layers along the a direction of the unit cell.[10,11] Examination of Figure 8 shows that a 180° jump of sections of the PPV chain would principally affect the interchain interaction in the a direction. A 180° jump of chain 1 would tilt the phenylene and vinylene groups of this chain toward chain 3 but would have little effect on chain 2, which is coplanar. Such a jump might be accompanied by an axial shift of chains in the adjacent layer to relieve steric crowding, and axial disorder could reduce the energy difference between the two chain jump conformations. Cooperative chain jumps might be coupled to slip between adjacent layers in the a direction. These NMR data, however, provide no direct information about slip motion if it exists.

The rotation of ±38° implied by the diffusion mechanism would involve substantial disruption of the unit cell structure. Electron diffraction data at room temper-

ature and energy minimization calculations have shown that the setting angle is confined to a small range (56–68°).[10,11] The predominance of jumps over diffusion suggests that the unit cell structure and setting angle also remain well determined at high temperature. It should also be noted that the NMR data for PPV-d_2 are also inconsistent with a jump motion that interchanges the setting angle of adjacent layers (i.e., between chains 1 and 3 of Figure 8). Such a motion would cause a greater-than-observed averaging of the spectra of both PPV-d_2 and PPV-d_4.

PPV films are unusual in that they show both high crystallinity and substantial ring-flip motion.[13-15] We have previously suggested that ring-flip motion in PPV results from the particular paracrystalline disorder of the PPV unit cell.[14,15] In the past, ring-flip motion has been attributed to the amorphous and disordered boundary regions of semicrystalline polymers.[16] For example, the conjugated polymer, polyaniline, shows ^{2}H NMR spectra more consistent with the usual behavior of semicrystalline polymers (a population of static rings at all temperatures).[32] The NMR data presented here show that the phenylene ring flip of PPV is not an isolated motion but accompanies a substantial movement of the entire PPV chain. The disorder of the axial registry between chains provides a plausible mechanism for PPV chain jumps and may also provide a plausible mechanism for coupled ring flips.

Recent two- and three-dimensional ^{2}H NMR experiments have provided the opportunity to specify precisely the mechanism associated with local conformational changes within the crystalline regions of several vinyl polymers.[33,34] For PPV, these experiments are technically difficult because of the long T_1 at room temperature and the similarity of the fast and slow exchange line shapes. Anistropic relaxation data and line shapes from oriented samples provide an additional means for elucidating the mechanism of local chain motion, but it is anticipated that two-dimensional experiments could also specify the PPV chain defect mechanism more precisely.

Conclusions

The ^{2}H quadrupole echo NMR spectra and spin–lattice relaxation data confirm that the structure of PPV is similar to that of *trans*-stilbene. Spectra obtained at an elevated temperature show that the C–D bond motion has effective 2-fold symmetry about the chain axis. A 180° vinylene rotational jump is the simplest motion with these attributes. Small-angle rotational diffusion without a jump is inconsistent with the observed spectra. The ^{2}H spin–lattice relaxation data also support a jump model and indicate that the vinylene and phenylene jump-rate distributions are similar.

A 2-fold jump motion is a natural motion for the PPV chain, and a 2-fold disorder about the PPV chain axis is the simplest type of disorder associated with PPV paracrystallinity. This disorder may be related to the lack of axial registry that occurs for adjacent planes along the a axis of the unit cell. The actual mechanism of PPV chain motion may be more complex than a 2-fold jump and perhaps involve a particular coupled motion of phenylene and vinylene groups. However, any proposed model for PPV motion should have the effective 2-fold symmetry about the chain axis, which is evident from high-temperature ^{2}H spectra.

Acknowledgment. We thank Lothar Frank for helpful discussions. This work was supported by AFOSR Grant 91-0010. J.H.S. thanks Lockheed Corp. for additional financial support.

References and Notes

(1) Wessling, R. A.; Zimmermann, R. G. U.S. Patent 3,401,152, 1968; U.S. Patent 3,706,677, 1972.
(2) Gagnon, D. R.; Capistran, J. D.; Karasz, F. E.; Lenz, R. W.; Antoun, S. *Polymer* **1987**, *28*, 567.
(3) Machado, J. M.; Karasz, F. E.; Kovar, R. F.; Burnett, J. M.; Druy, M. A. *New Polym. Mater.* **1989**, *1*, 189.
(4) Murase, I.; Ohnishi, T.; Noguchi, T.; Hirooka, M. *Polym. Commun.* **1984**, *25*, 327.
(5) Machado, J. M.; Masse, M. A.; Karasz, F. E. *Polymer* **1989**, *30*, 1992.
(6) Singh, B. P.; Prasad, P. N.; Karasz, F. E. *Polymer* **1988**, *29*, 1941.
(7) Bradley, D. D. C.; Friend, R. H.; Lindenberger, H.; Roth, S. *Polymer* **1986**, *27*, 1709.
(8) Machado, J. M. Ph.D. Dissertation, University of Massachusetts, Amherst, MA, 1989.
(9) Bradley, D. D. C. *J. Phys. D: Appl. Phys.* **1987**, *20*, 1389.
(10) Granier, T.; Thomas, E. L.; Gagnon, D. R.; Karasz, F. E.; Lenz, R. W. *J. Polym. Sci., Part B: Polym. Phys.* **1986**, *24*, 2793.
(11) Granier, T.; Thomas, E. L.; Karasz, F. E. *J. Polym. Sci., Part B: Polym. Phys.* **1989**, *27*, 469.
(12) Masse, M. A.; Martin, D. C.; Thomas, E. L.; Karasz, F. E.; Petermann, J. H. *J. Mater. Sci.* **1989**, *25*, 311.
(13) Simpson, J. H.; Rice, D. M.; Karasz, F. E. *Macromolecules* **1992**, *25*, 2099.
(14) Simpson, J. H.; Egger, N.; Masse, M. A.; Rice, D. M.; Karasz, F. E. *J. Polym. Sci., Part B: Polym. Phys.* **1990**, *28*, 1859.
(15) Simpson, J. H.; Rice, D. M.; Karasz, F. E. *J. Polym. Sci., Part B, Polym. Phys.* **1992**, *30*, 11.
(16) Jelinski, L. W. In *High Resolution NMR Spectroscopy of Synthetic Polymers in Bulk*; Komoroski, R. A., Ed.; VCH: Weinheim, FRG, 1986.
(17) Rice, D. M.; Wittebort, R. J.; Griffin, R. G.; Meirovitch, E.; Stimson, E. R.; Meinwald, Y. C.; Freed, J. H.; Scheraga, H. A. *J. Am. Chem. Soc.* **1981**, *103*, 7707.
(18) Griffin, R. G.; Beshah, K.; Ebelhauser, R.; Huang, T. H.; Olejniczak, E. T.; Rice, D. M.; Siminovitch, D. J.; Wittebort, R. J. In *The Time Domain in Surface and Structural Dynamics*; Long, G. J., Grandejeon, F., Eds.; Kluwer: New York, 1988; pp 81–105.
(19) Thomas, A. F. *Deuterium Labelling in Organic Chemistry*; Appleton: New York, 1976; pp 83–85.
(20) Liang, W.; Rice, D. M.; Karasz, F. E., submitted for publication in *Polym. Commun.*
(21) Opella, S. J.; Frey, M. H. *J. Am. Chem. Soc.* **1979**, *101*, 5854.
(22) Rice, D. M.; Meinwald, Y. C.; Scheraga, H. A.; Griffin, R. G. *J. Am. Chem. Soc.* **1987**, *109*, 1636.
(23) Cholli, A. L.; Dumais, J. J.; Engle, A. K.; Jelinski, L. W. *Macromolecules* **1984**, *17*, 2399.
(24) Wittebort, R. J.; Olejniczak, E. T.; Griffin, R. G. *J. Chem. Phys.* **1987**, *86*, 5411.
(25) Pschorn, U.; Spiess, H. W.; Hisgen, B.; Ringsdorf, H. *Makromol. Chem.* **1986**, *187*, 2711.
(26) Spiess, H. W. In *Developments in Oriented Polymers-1*; Ward, I. M., Ed.; Applied Science Publishers: London, 1982.
(27) Finder, C. J.; Newton, M. G.; Allinger, N. L. *Acta. Crystallogr.* **1974**, *B30*, 411.
(28) Torchia, D. A.; Szabo, A. *J. Magn. Reson.* **1982**, *49*, 107.
(29) Wittebort, R. J.; Szabo, A. *J. Chem. Phys.* **1978**, *69*, 1722.
(30) Fleming, W. W.; Fyfe, C. A.; Lyerla, J. R.; Vanni, H.; Yannoni, C. A. *Macromolecules* **1980**, *13*, 460.
(31) Boyd, R. H. *Polym. Rev.* **1985**, *26*, 323.
(32) Kaplan, S.; Conwell, E. M.; Richter, A. F.; MacDiarmid, A. G. *Macromolecules* **1989**, *22*, 1669.
(33) Schaefer, D.; Spiess, H. W.; Suter, V. W.; Fleming, W. W. *Macromolecules* **1990**, *23*, 3431.
(34) Hirschinger, J.; Schaefer, D.; Spiess, H. W.; Lovinger, A. J. *Macromolecules* **1991**, *24*, 2428.